ROYAL SOCIETY OF CHEMISTRY

PAPER

Check for updates

Novel chemical recycling process of REBCO materials showcased on TSMG-processed waste

Jan Sklenka,[a] Ondřej Jankovský,[a] Tomáš Hlásek[ab] and Filip Antončík ⓘ ⋆[ab]

Due to the increasing production of rare-earth barium copper mixed oxide (REBCO) superconductors, a significant amount of REBCO waste is produced. REBCO waste contains expensive rare earth elements and noble metals, as well as elements that can be hazardous to the environment if not handled properly. Therefore, it is important to develop a novel general recycling process for the production of fully-recycled single-domain REBCO bulks. In this contribution, YBCO waste was processed by chemical dissolution of YBCO waste in concentrated nitric acid, followed by precipitation and calcination steps to produce recycled YBCO precursor powder. Subsequently, the recycled precursor was utilized in the production of YBCO bulks by top-seeded melt growth. Single-domain YBCO bulks, grown exclusively from the recycled precursor, were successfully prepared. The analysis focused on their phase and elemental composition, as well as on their microstructure and key superconducting properties. The results demonstrate the feasibility of a closed production cycle for YBCO bulks, contributing to a more sustainable and eco-friendly approach to produce high-temperature superconductors. Even more importantly, this approach is designed to easily process other types of REBCO waste such as sputtering targets, granulates and possibly even thin-film superconducting tapes.

1. Introduction

High-temperature superconductors (HTSs) possess unique properties that make them indispensable in advanced applications such as maglev trains or medical imaging.[1–3] An important group of HTS materials is rare-earth barium copper mixed oxides (REBCO; RE = Y, Gd, Eu, Sm, *etc.*).[4] In REBCO systems, the most important phase is the superconducting $REBa_2Cu_3O_{7-\delta}$ (RE-123) phase, which is often accompanied by the non-superconducting RE_2BaCuO_5 (RE-211) phase.[5,6]

REBCO materials can be manufactured into several different forms based on the desired functions of the materials. For example, a thin layer of superconductive material can be grown/deposited on a suitable substrate producing thin-film coated conductors which are then made into a coil to serve as a source of high magnetic field in NMR as well as in MRI or other devices.[7,8] Another REBCO form, single-domain superconducting bulks, can be produced by various melt-growth processes.[9] Such bulks are used to trap strong magnetic fields or for self-stabilizing magnetic levitation (through quantum locking).[10,11] Traditionally, superconducting bulks are used in the production

of high-speed bearings or maglev trains, but nowadays they are showing great potential in the growing field of energy storage, where they can be used to manufacture levitating flywheels.[12,13]

Single-domain superconducting bulks can be produced by various methods. The two most common methods are top-seeded melt growth (TSMG) and top-seeded infiltration growth (TSIG).[14] In the TSMG method, precursor powder is pressed into a disc, on top of which a seed is placed.[15] During the subsequent heat treatment process above its peritectic temperature, the RE-123 phase decomposes to RE-211 and LP (liquid phase, $Ba_3Cu_5O_8$).[16] With the decreasing temperature during crystal growth, this reaction then reverses, allowing the re-formation of the RE-123 phase in the form of a single-domain crystal. However, in the case of the TSIG method, the precursor powder composed of RE-211 is pressed into a disc and the source of the LP is placed underneath the disc. During heat treatment, the LP infiltrates up into the disc resulting in the formation of the RE-123 phase and crystal growth occurs using the seed placed on top of the disc in either a one-step or a two-step process. Finally, a recently discovered novel method of crystal growth, "single direction melt growth (SDMG)", significantly improves the yield and robustness of the growth; however, a moderate amount of waste is produced during machining, as the misgrains near the seed and ungrowth region nearby the top of the bulk are ideally removed.[17–19]

Due to the delicate nature of the above-mentioned production processes, various defects sometimes occur in the produced

[a] *Department of Inorganic Chemistry, University of Chemistry and Technology Prague, Technická 5, 166 28, Prague 6, Czech Republic.*
E-mail: filip.antoncik@vscht.cz
[b] *CAN SUPERCONDUCTORS s.r.o., Ringhofferova 66, 251 68, Kamenice, Czech Republic*

Paper

bulks.[20] Secondary grains can grow in the bulk, significantly deteriorating its properties, which is why such bulks are most often discarded.[21–23] Another type of defect is large cracks in the volume of the bulk.[24,25] This is a problem mainly for bulks that are larger in diameter since during growth, the bulks are under higher stress due to high shrinkage during heat treatment. Furthermore, the overall defect rate grows exponentially with the size of the bulks, which further reduces the growth success rate. A substantial amount of precious materials has already been turned into waste through these failures during growth. For this reason, a recycling method for REBCO materials should be developed. Cardwell *et al.* solved the problem of secondary grains with their modified TSIG method, where they first flatten the top of the failed bulk and then they place a source of the liquid phase underneath the bulk to replace the liquid phase lost in the first melt-growth process.[26–28] Using this method however, only about 70–80% of superconducting properties (trapped field) of primarily grown bulks were achieved. It also does not address large cracks typical for large-diameter bulks, which while low in numbers consume disproportionally more powder with the increase in the bulk volume. Based on the current state-of-the-art methods, a universal recycling method has to be developed to efficiently re-use high-cost materials present in REBCO waste.

In this work, YBCO waste was processed by a novel recycling procedure that can be implemented on an industrial scale and that can be further modified for other more complex REBCO systems due to the presence of silver which is often used as an additive.[29] Our method is based on waste dissolution in concentrated nitric acid and subsequently the precipitation of the ions present in the solution. The precipitate was then used in a secondary precursor from which second-generation bulks were produced and characterized in detail.

2. Experimental

The following chemicals were used in this work: HNO_3 65% (p.a., Penta), KOH (p.a., 85%, Penta), H_2SO_4 96% (p.a., Penta), oxalic acid dihydrate (p.a., 99%, Penta), NH_4OH < 23% (p.a., Penta), CuO (p.a., Sigma–Aldrich, Czech Republic), $BaCO_3$ (99% +, Sigma–Aldrich, Czech Republic), and Y_2O_3 (99.99%, Sigma–Aldrich, Czech Republic). YBCO waste, supplied by commercial manufacturer CAN Superconductors, was also used.

In the industrial process of manufacturing YBCO bulks, precursor powder is prepared by solid-state synthesis from Y_2O_3, $BaCO_3$ and CuO. When producing recycled YBCO bulks, the precursor powder was prepared by using the product of recycling which was mixed with a minimal amount of raw materials (Y_2O_3, $BaCO_3$, and CuO) to achieve the correct stoichiometry for crystal growth. The desired ratio is 1.0 $YBa_2Cu_3O_x$:0.4 Y_2BaCuO_x (Y-123:Y-211 = 1.0 : 0.4). The recycled precursor powder was subsequently processed exactly as regular industrial precursor powder. The powder was calcined in one batch. In total, four calcinations were carried out between 850 °C and 880 °C (10 °C increments). Homogenization by

grinding was performed between steps. Afterwards, the precursor powder was uniaxially pressed using approximately 50 MPa of pressure into 32 mm diameter discs (42 g). These were then processed using the TSMG method under an air atmosphere with commercially available Nd-123 as seeds. The temperature profile used was as follows: heating to 900 °C in 3 h, heating to 930 °C in 1 h, heating to 1065 °C in 1 h, holding at 1065 °C for 1 h, cooling to 1010 °C in 15 min, cooling to 995 °C in 30 min, cooling to 991 °C in 1 h, crystal growth at a temperature of 991 °C for 30 h, crystal growth during cooling to a temperature of 987 °C in 20 h and subsequent natural cooling in a furnace. Successfully grown bulks were annealed in a flowing oxygen atmosphere to saturate the crystal lattice with oxygen at temperatures between 300 °C and 450 °C for 200 h. Finally, grown bulks were machined to a diameter of 28 mm and a height of 10 mm. On the other hand, defective bulks (those containing secondary grains or some other defects) were removed.

Selected recycled bulks with the highest levitation force and the lowest levitation force and one reference bulk from industrial production were cut in half. These bulks were cut perpendicularly to the square-shaped main grain and the surface of the cut was polished (see Fig. 1).

X-ray diffraction (XRD) was performed using a Bruker D8 ADVANCE device with Bragg–Brentano geometry. The radiation source is Cu K-α with the following parameters: λ = 0.15418 nm, U = 30 kV, and I = 30 mA. The data were obtained in the angular range of 5°–80° (2θ) with a step size of 0.02° (2θ). X'Pert HighScore Plus software was used to analyse the obtained data. The same software was used for the quantitative phase analysis using Rietveld analysis.

Optical microscopy of the samples was carried out with Navitar macro-optics (Rochester, United States) with an optical magnification of up to 110X. The photographs were taken with a Sony 2/3″ digital camera (resolution 5 Mpx). The samples were illuminated by a white LED circular lamp with individual adjustable segments. The NIS-Elements BR 5.21.02 software with extended depth of focus module (EDF) was used for displaying and analysing samples.

The levitation force was measured using an in-house designed device (Fig. 2) that is based on a load cell PT4000-50 kg with ± 0.1 N accuracy and a 24-bit ADC Data Acquisition system. A load cell physically connected to the permanent magnet measures the repulsion force between the permanent
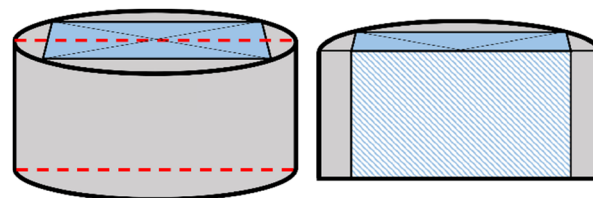

Fig. 1 Schematic drawing of how the bulks were cut. On the left, the whole bulk is pictured with the main grain in blue and the cut lines in red. On the right, the cut bulk is pictured with the area of focus (the main grain) indicated by hatching.
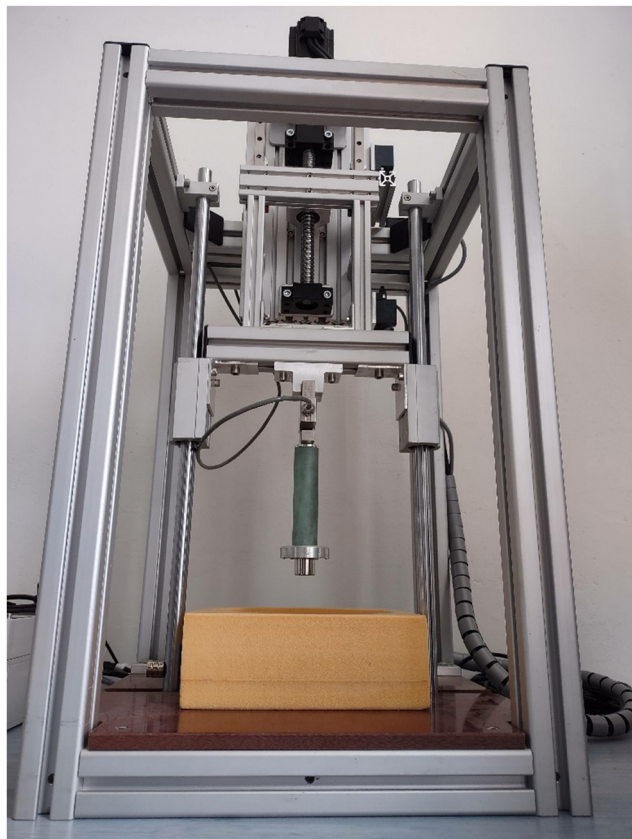
Fig. 2 A photograph of the used in-house designed device for levitation force.

magnet and the superconducting bulk. The measured bulk is cooled by submersion in liquid nitrogen in a zero field. Subsequently, a servo motor moves the permanent magnet towards the superconducting bulk and the levitation force is recorded every 0.1 mm. A permanent magnet (NdFeB, N52, d = 25 mm, h = 25 mm, with magnetic field B = 0.575 T) was used to measure the levitation at 77 K. The samples were cooled below the critical temperature in a zero external magnetic field.

The chemical composition of the recycled product was analyzed using ICP-AES by Mikroanalytisches Labor Pasher from the recycled product dissolved in nitric acid.

3. Results and discussion

The recycling process developed in this work is described in Fig. 3. The following points each correspond to one step in the picture.

1. The waste powder was sourced in the form of defective bulks from the REBCO manufacturer CAN SUPERCONDUCTORS s.r.o. and ground in a disk mill into a fine powder. Overall, 5 kg of commercial YBCO bulks was pulverized and processed.

2. YBCO waste was added to concentrated nitric acid in a ratio of 1 kg of YBCO waste to 2.5 l of concentrated HNO_3. The powder was added slowly and the mixture was stirred continuously
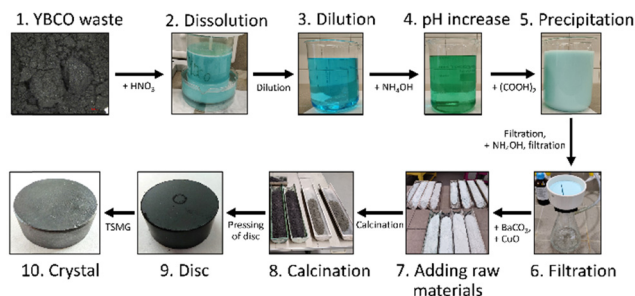

Fig. 3 Diagram of the recycling process.

because the waste dissolution was strongly exothermic. After adding all the waste, the mixture was allowed to stand for 24 h allowing the acid to completely dissolve any remaining YBCO. The obtained mixture consisted of Ba^{2+}, Cu^{2+}, Y^{3+} and NO^{3-} ions with some precipitated $Ba(NO_3)_2$ due to its low solubility.

3. The mixture was then diluted with distilled water until the solid intermediate product ($Ba(NO_3)_2$) was dissolved. The resulting volume of the mixture after this step was about 40 l per 1 kg of YBCO waste.

4. Subsequently, ammonium hydroxide was added to adjust the pH to slightly basic until a color change from blue to green was observed (approximately 1 l of ammonium hydroxide was added per 1 kg of YBCO waste).

5. If silver is present in the waste, it will be dissolved along with RE-Ba-Cu. Subsequently, it is selectively precipitated after the dilution by the addition of HCl in the form of AgCl and filtered. The filtered AgCl can be reduced to Ag_2O or metallic silver and reused.[29]

6. Oxalic acid was added to the solution (approximately 1.2 kg per 1 kg of YBCO waste), thereby precipitating most of the yttrium, copper and barium ions present in the solution in the form of respective oxalates: $Y_2(C_2O_4)_3$, $Ba(C_2O_4)$ and $Cu(C_2O_4)$.

7. The precipitate was separated by filtration as the product of the reaction. However, due to the significantly higher solubility of barium oxalate in comparison to yttrium and copper oxalates, a part of the remaining barium was precipitated in the second step to improve the yield and reduced waste of the recycling - ammonium hydroxide was added to the filtrate to raise the pH to precipitate a portion of dissolved Ba^{2+} ions out of the solution in the form of $Ba(NO_3)_2$ (approximately 0.5 l of ammonium hydroxide was added per 1 kg of YBCO waste). A second precipitate formed, which was then also separated by filtration and mixed with the first precipitate.

8. The mixed precipitate was purified by repeated washing in demineralized water and subsequently dried, weighed and analysed using ICP-AES. This dried powder is considered a product of recycling. In the remaining filtrate, the toxic Ba^{2+} ions present were converted to non-toxic $BaSO_4$ by reaction with H_2SO_4. $BaSO_4$ was a by-product of the method and was not processed further in this work.

9. The yield of this recycling process was 71%, determined as to the total weight of the dry RE-Ba-Cu-O mixture in comparison with input industrial waste (*i.e.* per one kg of YBCO waste, approximately 710 g of the RE-Ba-Cu-O mixture was recovered).

3328 | *J. Mater. Chem. C*, 2024, **12**, 3326–3332

This journal is © The Royal Society of Chemistry 2024

Paper

Through the presented data in the later section, it will be clear that the majority of losses can be attributed to the higher solubility of barium oxalate compared to other oxalates.

10. The precipitates were then mixed with CuO and BaCO$_3$ to achieve the ideal composition for crystal growth of Y$_{1.8}$Ba$_{2.4}$Cu$_{3.4}$O$_x$.

11. The resulting powder (recycled precursor) was then calcined and used for the growth of single-domain bulks by TSMG. The calcination process, TSMG growth, annealing and characterization are described in detail in the Experimental section.

YBCO waste used in this work consists of defective YBCO bulks ground in a disc mill. To determine the phase composition, X-ray diffraction was performed (see Fig. 4). Three phases were determined to be present: YBa$_2$Cu$_3$O$_7$ (Y-123, 01-070-6571), Y$_2$BaCuO$_5$ (Y-211, ICDD 00-038-1434) and CuO (ICDD 01-080-1917).[30–32] According to Rietveld analysis, the composition of the used YBCO waste is 65.8 wt% Y-123 phase, 32.4 wt% Y-211 phase and 1.7 wt% CuO. This composition differs from the ideal growth stoichiometry that the industrial precursor powder had. The ideal composition for YBCO crystal growth is found to be 1 Y-123 : 0.4 Y-211 (78.4 wt% Y-123, 21.4 wt% Y-211). The corresponding elemental stoichiometry of this ideal-for-growth composition is shown in Table 1 together with the stoichiometry of YBCO waste. The difference in the two compositions originates during the growth of the YBCO bulks, during which some liquid phase Ba$_3$Cu$_5$O$_8$ is lost.

As mentioned before, the difference between the two compositions originates during the TSMG process. In standard industrial YBCO bulk production, the growth stoichiometry is achieved by mixing raw materials in the correct ratio. The composition data for YBCO waste were obtained from XRD measurement by Rietveld analysis. The obtained stoichiometry corresponds to 51.7 wt% Y-123, 37.1 wt% Y-211 and 11.2 wt% CuO.
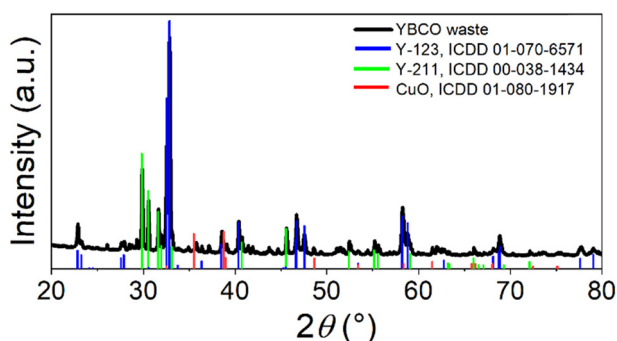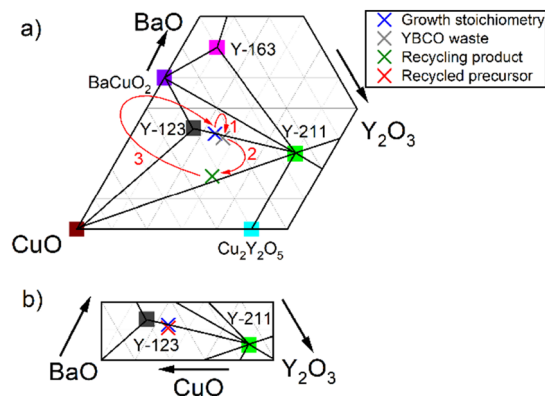

Fig. 5 Sub-section of the YBCO phase diagram (a) with important points of closed production cycle highlighted and (b) with a close-up of the recycled precursor composition. Compositions of each point on the diagram are determined as follows: the growth stoichiometry is the stoichiometry used by CAN Superconductors in their production; the YBCO waste composition was determined from Rietveld analysis; and compositions of the recycling product as well as the recycled precursor were determined using an ICP-AES obtained from Mikroanalytisches Labor Pasher.

In Fig. 5, YBCO ternary phase diagrams can be seen describing the overall process. The top diagram (Fig. 5a) shows the changes in the elemental composition, where the blue cross marks the desired stoichiometry for the crystal growth:

Arrow 1 shows how the composition of the defective YBCO bulks shifts from the original position at the link between Y-123 and Y-211 phases to an area with less barium and copper contents due to the loss of the liquid phase Ba$_3$Cu$_5$O$_8$ during crystal growth.

Arrow 2 leads from the composition of YBCO waste to the region of the recycling product's composition. This shift happens due to the loss of unprecipitated ions in the solution. The composition of the recycling product was measured by ICP-AES.

Arrow 3 then indicates a shift in the composition that starts from the region of the recycling product and by mixing the recycling product with raw materials the resulting recycled precursor again has the composition suitable for growing YBCO crystals. The correct amount of raw materials was determined from the ICP-AES composition data of the recycling product. To obtain the desired growth stoichiometry, only a minimal amount of BaCO$_3$ and CuO was added (Y$_2$O$_3$ was not added as it was in excess). The stoichiometric ratio of elements (obtained by highly precise ICP-AES) in the product and recycled precursor is described in Table 2. The exact composition of the recycled precursor in the magnified section of the

Fig. 4 Diffraction patterns of YBCO waste.

Table 1 Comparison of metal stoichiometry in YBCO crystal growth stoichiometry and YBCO waste

	Growth stoichiometry	YBCO waste
Y	1.8	1.80
Ba	2.4	2.01
Cu	3.4	2.91

Table 2 Comparison of metal stoichiometry in the recycling product, recycled precursor, and growth stoichiometry

		ICP-AES	
	Growth stoichiometry	Recycling product	Recycled precursor
Y	1.8	1.80	1.80
Ba	2.4	1.06	2.28
Cu	3.4	3.17	3.38

YBCO phase diagram is shown separately for clarity in the bottom part of Fig. 5b showing that the obtained composition is very close to the ideal composition.

In addition to the elemental composition, the phase composition of the recycled precursor was determined by XRD. The data obtained in this way were compared with the reference data measured by the analysis of the precursor used in the industrial production of YBCO bulks (see Fig. 6). Two phases were confirmed to be present in both samples: $YBa_2Cu_3O_7$ (Y-123, ICDD 01-078-2274) and Y_2BaCuO_5 (Y-211, ICDD 01-080-0770).[33,34] The recycled precursor showed high phase composition agreement with the reference precursor.

The recycled precursor was used for the preparation of YBCO single-domain crystals using the TSMG method. The defect rate in the recycled bulks was very similar to the defect rate in commercial YBCO bulk production. Non-defective bulks were selected for further analysis. Fig. 7 shows recycled YBCO bulks. In most bulks, the main crystal grain has not grown all the way to the edges of the bulk. This means a smaller volume of the ordered microstructure, which in return yields worse superconductive properties of the bulks.
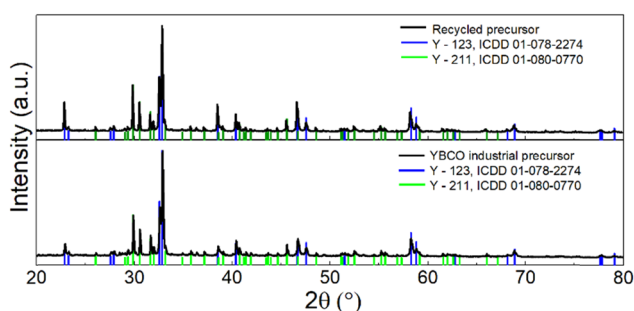
Each of the recycled bulks was marked with a letter and in the next step, their levitation force was measured (see Fig. 8). From Fig. 8a, we can see the experimentally obtained data between 1.9 mm and 3 mm for recycled bulks. The levitation force increases with the decreasing distance from the bulk. An exponential fit $F = F_{max} + A\exp(Bd)$ was applied to the obtained data in accordance with the current praxis.[35] Fitted curves showed the maximal levitation force at the bulk surface. These maximal levitation forces of each bulk are seen in Fig. 8b. An average maximal force was determined to be 40.32 ± 6.37 N. This means that on average the recycled bulks reached about 50% of the industry standard for the highest grade bulks (80 N). Based on the data, the following bulks were selected for further detailed analysis: the best bulk (M, $F_{max} = 52.4$ N), the average bulk (F, $F_{max} = 40.01$ N), and the worst bulk (J, $F_{max} = 26.01$ N). A bulk from industrial production was analysed together with these selected bulks as a reference.

The microstructure of selected recycled bulks was studied (see Fig. 9). The best bulk (M, with highest levitation force), the worst bulk (J, with lowest levitation force), the average bulk (F, with levitation force close to the calculated average), as well as the standard industry production bulk reference (REF), were studied by optical microscopy. The bulks were cut into half perpendicularly to the square-shaped main grain before this
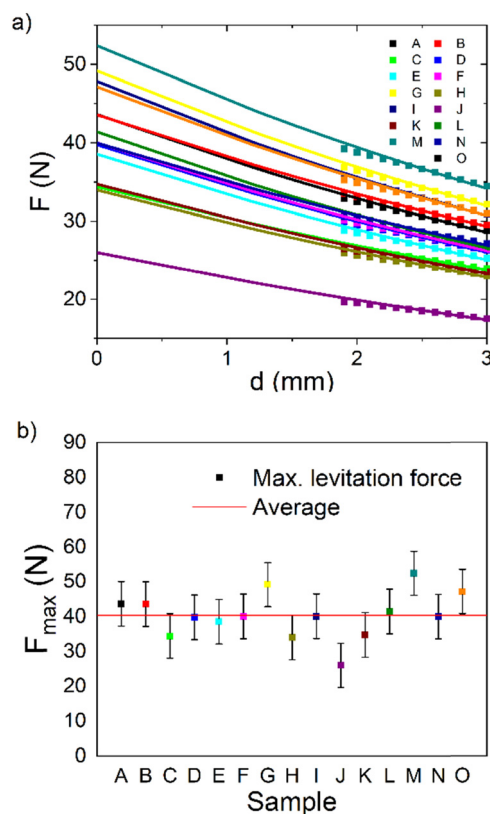

Fig. 6 Comparison of the XRD data of the recycled precursor with the reference data (commercial YBCO-bulk precursor).

Fig. 7 Recycled YBCO bulks. One bulk was cut due to the presence of secondary grains. The bulks were marked with letters A–O. From left to right, in the first row are bulks A–E, in the second row are bulks F–I and in the third row are bulks H–O.

Fig. 8 Levitation force (F) of recycled YBCO bulks (a) and calculated maximal levitation forces (F_{max}) at the surface of the bulk (b). Each letter represents a sample, and all samples were prepared in the same way, though they differ in their performance (which is expected for all TSMG prepared samples).

3330 | *J. Mater. Chem. C*, 2024, **12**, 3326–3332

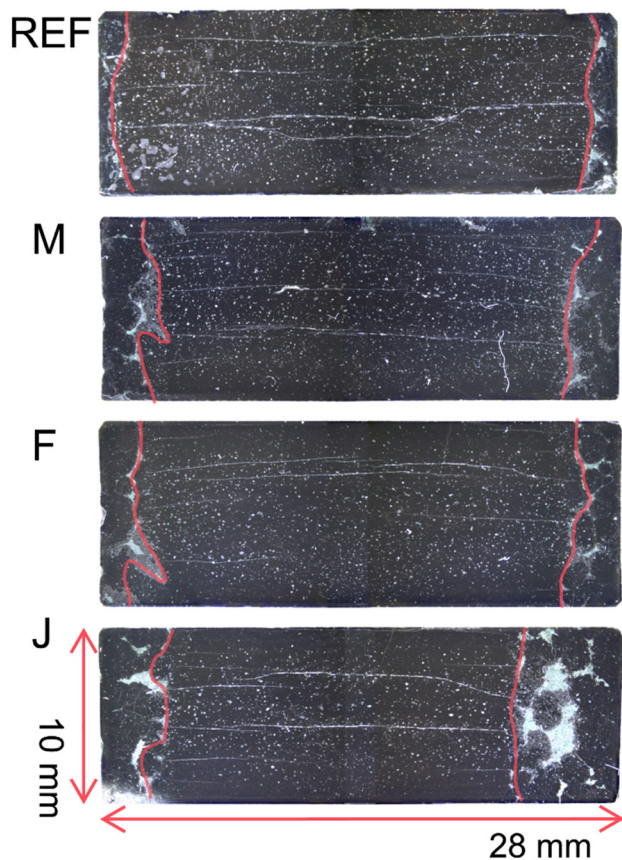This journal is © The Royal Society of Chemistry 2024

Fig. 9 Optical microscopy analysis of the selected bulks. Borders of the main grain are highlighted using red colour. From top to bottom: the industrial reference bulk (REF), the best bulk (M), the average bulk (F), and the worst bulk (J).
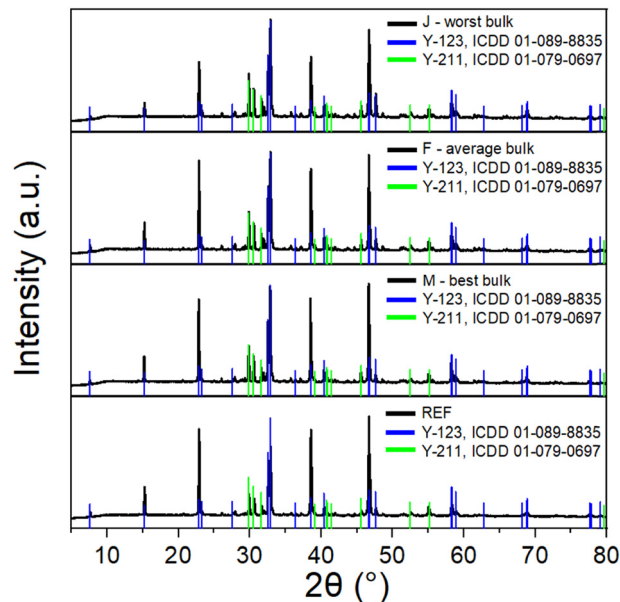

Fig. 10 Comparison of the XRD data of ground recycled bulks with the ground reference industrial bulk. From top to bottom: the worst bulk (J), the average bulk (F), the best bulk (M) and the industrial reference bulk (REF).

4. Conclusions

In this work, a new general recycling process designed for REBCO waste was developed, specifically focusing on the production of single-domain fully-recycled YBCO bulks by the TSMG method. The recycling process utilizes a combination of chemical dissolution, precipitation, and calcination steps to transform YBCO waste into recycled precursor powder suitable for crystal growth. The recycled precursor powder was then treated similarly to regular industrial precursor powder and processed through the TSMG method to produce YBCO bulks. The overall efficiency of the recycling process was evaluated, showing an overall yield of 71% in laboratory-scale experiments, which means that 71% of metals (Y + Ba + Cu) can be fully recycled. The vast majority of losses are in barium (in the form of non-toxic $BaSO_4$), which is very cheap in comparison with rare earth and copper; therefore, the losses do not impact the overall economy of the recycling process, which is crucial to its eventual implementation into the REBCO production chain.

Using the product of recycling doesn't seem to inhibit crystal growth: the defect rate during TSMG in the recycled YBCO bulks is found to be similar to that in commercial YBCO bulk production, suggesting that no impurities which negatively impact TSMG were introduced during recycling. The levitation force of the recycled YBCO bulks, while currently at approximately 50% of the industry standard for the highest-grade bulks, shows potential for improvement through further optimization. This result is not surprising, given that the bulks were grown exclusively out of the recycled precursor. Furthermore, the recycled bulks were grown together with bulks from normal production; therefore, the heat-treatment profile was not optimized for recycled composition. Given the notoriously high sensitivity of TSMG, the achieved results show great

measurement, as can be seen in Fig. 2. Typically, during the TSMG process, a single-domain crystal is formed; however, the size of the crystal varies significantly. Micrographs confirmed a correlation between the size of the main grain of the crystal and the levitation force. The bigger the grain, the higher the volume of the crystal and therefore also the higher the levitation force.[12,36] The bulks show the typical microstructure of TSMG-processed REBCO bulks, with horizontal cracks, small defects, bubbles and voids. The microstructural data suggest that there are no issues with the TSMG growth itself, which could arise as a result of contamination introduced during recycling.

Let us note that the borders of the crystals were highlighted using red color for better visualization.

In the next step, the second half of the bulk was crushed and analysed using XRD. The phase composition of the different bulks was very similar (see Fig. 10), which confirmed that the developed recycling process did not influence the phase composition, which is crucial to achieve sufficient superconducting properties. All samples contained $YBa_2Cu_3O_7$ (Y-123, ICDD 01-089-8835) as well as Y_2BaCuO_5 (Y-211, ICDD 01-079-0697).[37,38] Preferential orientation of (00l) reflections in the Y-123 was observed due to its layered structure.

This journal is © The Royal Society of Chemistry 2024

J. Mater. Chem. C, 2024, **12**, 3326–3332 | **3331**

promise. We plan to carry out further research, where the recycled powder is mixed with a larger amount of raw precursors, which will reflect the probable use in industrial settings.

Based on the obtained results, we believe that such an optimized recycling process will enable a closed production cycle for REBCO bulks, contributing to more sustainable high-temperature superconductor manufacturing. Such an approach will lead to a significant decrease in raw material consumption, leading to significant economic and eco-friendly benefits.

Author contributions

Jan Sklenka: writing – original draft and investigation; Ondřej Jankovský: writing – review and editing, conceptualization, and supervision; Tomáš Hlásek: validation and data curation; Filip Antončík: writing – review and editing, conceptualization, methodology, and investigation.

Conflicts of interest

There are no conflicts to declare.

Acknowledgements

Notes and references

1 K. Bennemann and J. B. Ketterson, *Superconductivity*, Springer, 2008, pp. 3–26.
2 G. Sotelo, R. De Oliveira, F. Costa, D. Dias, R. De Andrade and R. Stephan, *IEEE Trans. Appl. Supercond.*, 2014, **25**, 1–5.
3 R. Aarnink and J. Overweg, *Europhys. News*, 2012, **43**, 26–29.
4 Y. Chen, X. Cui and X. Yao, *Prog. Mater. Sci.*, 2015, **68**, 97–159.
5 C. Chu, *Proc. Natl. Acad. Sci. U. S. A.*, 1987, **84**, 4681.
6 V. Bartůněk, J. Luxa, D. Sedmidubský, T. Hlásek and O. Jankovský, *J. Mater. Chem. C*, 2019, **7**, 13010–13019.
7 S. Mukoyama, A. Nakai, H. Sakamoto, S. Matsumoto, G. Nishijima, M. Hamada, K. Saito and Y. Miyoshi, 2018.
8 S. Kar, W. Luo and V. Selvamanickam, *IEEE Trans. Appl. Supercond.*, 2017, **27**, 1–4.
9 A. Campbell and D. Cardwell, *Cryogenics*, 1997, **37**, 567–575.
10 K. Ma, Y. Postrekhin and W. Chu, *Rev. Sci. Instrum.*, 2003, **74**, 4989–5017.
11 M. D. Ainslie and H. Fujishiro, *Supercond. Sci. Technol.*, 2015, **28**, 053002.
12 F. Werfel, U. Floegel-Delor, R. Rothfeld, T. Riedel, B. Goebel, D. Wippich and P. Schirrmeister, *Supercond. Sci. Technol.*, 2011, **25**, 014007.
13 S. Wang, J. Wang, C. Deng, Y. Lu, Y. Zeng, H. Song, H. Huang, H. Jing, Y. Huang and J. Zheng, *IEEE Trans. Appl. Supercond.*, 2007, **17**, 2067–2070.
14 S. Umakoshi, Y. Ikeda, A. Wongsatanawarid, C.-J. Kim and M. Murakami, *Phys. C*, 2011, **471**, 843–845.
15 S. Marinel, J. Wang, I. Monot, M. Delamare, J. Provost and G. Desgardin, *Supercond. Sci. Technol.*, 1997, **10**, 147.
16 R. Cloots, T. Koutzarova, J.-P. Mathieu and M. Ausloos, *Supercond. Sci. Technol.*, 2004, **18**, R9.
17 P. Diko, K. Zmorayová, T. Motoki and J. Shimoyama, *Ceram. Int.*, 2023, **49**(23), 39280–39288.
18 T. Motoki, R. Sasada, T. Tomihisa, M. Miwa, S.-I. Nakamura and J.-I. Shimoyama, Development of homogeneous and high-performance REBCO bulks with various shapes by the single-direction melt growth (SDMG) method, *Supercond. Sci. Technol.*, 2022, **35**(9), 094003.
19 T. Motoki, M. Semba and J.-I. Shimoyama, Direct fabrication of high-quality ring-shaped REBa$_2$Cu$_3$O$_y$ bulk magnets by the single-direction melt growth (SDMG) method, *Appl. Phys. Express*, 2023, **16**(9), 095501.
20 P. Diko, *Supercond. Sci. Technol.*, 2000, **13**, 1202.
21 F. Sandiumenge, N. Vilalta, X. Obradors, S. Piñol, J. Bassas and Y. Maniette, *J. Appl. Phys.*, 1996, **79**, 8847–8849.
22 U. Floegel-Delor, T. Riedel, P. Schirrmeister, R. Koenig, V. Kantarbar, M. Liebmann and F. Werfel, Strictly application-oriented REBCO bulk fabrication, *J. Phys.: Conf. Ser.*, 2020.
23 F. Antončík, M. Lojka, T. Hlásek, V. Plecháček and O. Jankovský, *Ceram. Int.*, 2022, **48**, 5377–5385.
24 P. Diko, N. Pelerin and P. Odier, *Phys. C*, 1995, **247**, 169–182.
25 P. Diko, W. Gawalek, T. Habisreuther, T. Klupsch and P. Gornert, *Appl. Supercond.*, 1995, **148**, 119–122.
26 Y. Shi, D. K. Namburi, M. Wang, J. Durrell, A. Dennis and D. Cardwell, *J. Am. Ceram. Soc.*, 2015, **98**, 2760–2766.
27 J. V. Congreve, Y. H. Shi, A. R. Dennis, J. H. Durrell and D. A. Cardwell, *J. Am. Ceram. Soc.*, 2016, **99**, 3111–3119.
28 D. K. Namburi, K. Singh, K. Y. Huang, S. Neelakantan, J. H. Durrell and D. A. Cardwell, *J. Eur. Ceram. Soc.*, 2021, **41**, 3480–3492.
29 F. Antončík, M. Lojka, T. Hlásek, J. Sklenka, O. Jankovský and D. Sedmidubský, *IEEE Trans. Appl. Supercond.*, 2023, **33**, 1–5.
30 X. Wu, F. Wang, S. Nie, J. Liu, L. Yang and S. Jiang, *Phys. C*, 2000, **339**, 129–136.
31 W. Wong-Ng, H. F. McMurdie and B. Paretzkin, *et al.*, *Powder Diffr.*, 1987, **2**(3), 191–202.
32 S. Asbrink and A. Waskowska, *J. Phys.: Condens. Matter*, 1991, **3**, 8173.
33 J. Capponi, C. Chaillout, A. Hewat, P. Lejay, M. Marezio, N. Nguyen, B. Raveau, J. Soubeyroux, J. Tholence and R. Tournier, *Europhys. Lett.*, 1987, **3**, 1301.
34 B. Hunter, S. Town, R. Davis, G. Russell and K. Taylor, *Phys. C*, 1989, **161**, 594–597.
35 O. Jankovský, F. Antončík, T. Hlásek, V. Plecháček, D. Sedmidubský, Š. Huber, M. Lojka and V. Bartůněk, *J. Eur. Ceram. Soc.*, 2018, **38**, 2541–2546.
36 P. Diko, *Phys. C*, 2006, **445**, 323–329.
37 X. Wu and J. Gao, *Phys. C*, 1999, **315**, 215–222.
38 S. Sato and I. Nakada, *Acta Crystallogr., Sect. C: Cryst. Struct. Commun.*, 1989, **45**, 523–525.

3332 | *J. Mater. Chem. C*, 2024, **12**, 3326–3332

This journal is © The Royal Society of Chemistry 2024